ADVANCED FUNCTIONAL MATERIALS
www.afm-journal.de

www.MaterialsViews.com

Comparative Study of the N-Type Doping Efficiency in Solution-processed Fullerenes and Fullerene Derivatives

*Stephan Rossbauer, Christian Müller, and Thomas D. Anthopoulos**

Molecular doping of organic semiconductors and devices represents an enabling technology for a range of emerging optoelectronic applications. Although p-type doping has been demonstrated in a number of organic semiconductors, efficient n-type doping has proven to be particularly challenging. Here, n-type doping of solution-processed C_{60}, C_{70}, [60]PCBM, [70]PCBM and indene-C_{60} bis-adduct by 1*H*-benzimidazole (N-DMBI) is reported. The doping efficiency for each system is assessed using field-effect measurements performed under inert atmosphere at room temperature in combination with optical absorption spectroscopy and atomic force microscopy. The highest doping efficiency is observed for C_{60} and C_{70} and electron mobilities up to ≈2 cm^2/Vs are obtained. Unlike in substituted fullerenes-based transistors where the electron mobility is found to be inversely proportional to N-DMBI concentration, C_{60} and C_{70} devices exhibit a characteristic mobility increase by approximately an order of magnitude with increasing dopant concentration up to 1 mol%. Doping also appears to significantly affect the bias stability of the transistors. The work contributes towards understanding of the molecular doping mechanism in fullerene-based semiconductors and outlines a simple and highly efficient approach that enables significant improvement in device performance through facile chemical doping.

1. Introduction

Organic semiconductors continue to attract significant interest due to their unique and highly tuneable physical characteristics and their tremendous potential for use in a range of applications including light emitting diodes (OLED),[1] organic solar cells[2] and thin-film transistors (TFT).[3] While a large number of high mobility hole-transporting materials have been synthesised and implemented in TFTs, electron transporting semiconductors and devices are relatively sparse.[4,5] To this end, fullerenes and particularly C_{60} are amongst the best performing electron transporting molecular semiconductors known to date and electron mobilities in the range of 6–11 cm^2/Vs have been reported.[6,7] Unfortunately, the best performing C_{60} transistors are commonly fabricated via vacuum-based techniques such as sublimation,[6,8] with only a few exceptions,[7,9–11] while to date there is no report on C_{70} devices fabricated via solution-based techniques. This processing limitation is primarily imposed by the limited solubility of substituted fullerenes in common organic solvents. Methanofullerene such as [6,6]-Phenyl C_{61} butyric acid methyl ester ([60]PCBM), [6,6]-Phenyl C_{71} butyric acid methyl ester ([70]PCBM) and indene-C_{60} bis-adduct (ICBA) avoid this problem as they are highly soluble and have already shown promise for use in organic solar cells,[12] TFTs and integrated logic circuits.[13] Despite these recent developments, however, fabrication of high performance e-transporting fullerene TFTs via solution processing remains a significant challenge.

In addition to the search and development of new molecular semiconductors, different methods for doping organic compounds have also been investigated in an effort to overcome inherit materials limitations and to improve the overall device/system performance. Advantages of doping include the addition of mobile (free) charge carriers, which can result in the filling of traps and hence improve the overall charge transport, as well as in the decrease of the barrier for charge carrier injection from the conductive electrodes into the molecular semiconductor. Unfortunately, these advantages come at a price since the introduction of an additional molecular species can disrupt the packing of the host semiconductor and hence induce structural defects. Furthermore, in closely packed (crystalline) systems a hybridization of orbitals of the host and the dopant materials can cause energetic disorder and hinder charge transport.[14] As every additional dopant molecule increases the structural/energetic disorder in the film, it is desirable for the dopant to be efficient, i.e., all dopant molecules donate charge carriers to the semiconductor. To date, a number of extrinsically doped organic systems have been reported in the literature[15] with the best example being the p-doped organic interlayer technology used extensively in state-of-the-art OLEDs[16] and OPVs.[17]

S. Rossbauer, Prof. T. D. Anthopoulos
Department of Physics and Center for Plastic Electronics
Imperial College London
London SW7 2BW, UK
E-mail: thomas.anthopoulos@imperial.ac.uk
Dr. C. Müller
Department of Chemical and Biological Engineering/
Polymer Technology
Chalmers University of Technology
412 96, Göteborg, Sweden

DOI: 10.1002/adfm.201401842

On the contrary, n-type dopants and the associated physical processes, have been little investigated and as such are still in their infancy.[18–21]

For n-type doping in an organic semiconductor to occur, the energetic structure of the dopant must allow for electron transfer from the dopant to the semiconductor. In the case of molecular dopants, this would require the ionization energy of the dopant to be lower than the electron affinity of the semiconducting host material. Since the electron affinity in most organic electron transporting semiconductors is fairly low (–3.5 eV to –4.5 eV),[22] candidate n-type dopants should be even more unstable towards atmospheric oxidants (e.g., water, oxygen). This is the primary reason why development of organic n-type dopants has been particularly challenging. In recent years organometallic[18,20,23,24] as well as all-organic molecular compounds have been attracting significant attention due to their potential as n-type dopants. One method to create air-stable dopants is to combine the electron transfer from the dopant to the host matrix with a chemical reaction. Notably, (4-(1,3-dimethyl-2,3-dihydro-1*H*-benzoimidazol-2-yl) phenyl)dimethylamine (N-DMBI), and other DMBI derivatives, have successfully been utilized as efficient and relatively stable n-dopants in cross-linked thiophenenapthalenediimide copolymers[25], poly(phenylene vinylene)[26] as well as in [60]PCBM[27] and C_{60}[28] films processed via solution-processing and co-evaporation, respectively. The initial dopant compound is air-stable and only after cleaving a C-H bond in solution a hydride transfer to the fullerene is possible, which leads to a net charge transfer into the host semiconducting molecule.[29] So when compared to conventional electron transferring dopants, instead of the electron affinity being the main deciding factor for selection of a suitable semiconducting host material for a given dopant, the hydride affinity and the reaction kinetics of the dopant with the host material become essential as well. Therefore, n-type molecular dopants that rely on the hydride transfer mechanism are particularly attractive as they could potentially combine the much desired chemical stability with high doping efficiency.

Here we report on the use of N-DMBI as an efficient n-dopant for a number of electron transporting unsubstituted and substituted fullerenes processed from solution. The doping efficiency in each system was assessed via field-effect measurements performed using optimised transistor architectures at room temperatures in combination with optical absorption spectroscopy and atomic force microscopy measurements. Based on these measurements we show that the n-doping process is orders of magnitude more efficient in the case of unsubstituted C_{60} and C_{70} fullerenes as compared to their substituted counterparts. Most importantly, n-doped C_{60} and C_{70} transistors exhibit significantly enhanced electron mobility (≈2 cm^2/Vs) and greatly improved bias stress stability. Unlike unsubstituted fullerenes, the performance characteristics of fullerene derivatives based transistors are found to degrade with increasing dopant concentration. The work provides the first experimental evidence on the differences of doping efficiency of fullerene-based transistors and its relation to the molecular structure of these much promising molecular semiconductors.

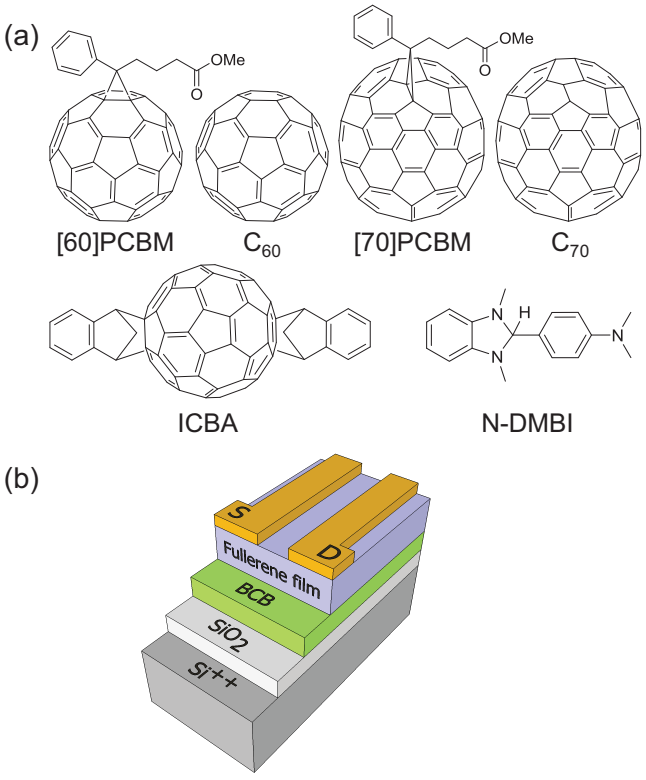

Figure 1. a) Chemical structures of the different fullerenes and fullerene derivatives employed in this work together with the n-type dopant N-DMBI b) Schematic representation of the bottom-gate, top-contact (BG-TC) transistor architecture used.

2. Results and Discussion

The chemical structures of the different fullerenes and fullerene derivatives employed in this work are shown in **Figure 1**a while a schematic of the bottom-gate, top-contact (BG-TC) transistor architecture used for electrical characterisation is shown in Figure 1b. The output characteristics of the different fullerene-based transistors fabricated in this work are shown in Figure S1 (Supporting Information). Each device shows a linear dependence of the drain current (I_D) on the drain-source voltage (V_D) in the low voltage range suggesting the formation of an Ohmic-like contact between the aluminium (Al) source/drain electrode and the semiconducting films—a characteristic feature indicating efficient electron injection from Al to the LUMO level of the semiconductor. For high V_D the channel current saturates in accordance with the gradual channel approximation model therefore justifying its use for analysing the device data obtained in this work.

Figure 2 displays sets of representative transfer characteristics for [60]PCBM, [70]PCBM and ICBA transistors for different molar concentrations of N-DMBI. Devices based on all three semiconducting molecules show an increase in the channel OFF-current with increasing N-DMBI concentration. The latter observation is attributed to the increased bulk conductivity of the fullerene layer due to the increased concentration of free electrons across the semiconducting layer. A similar doping

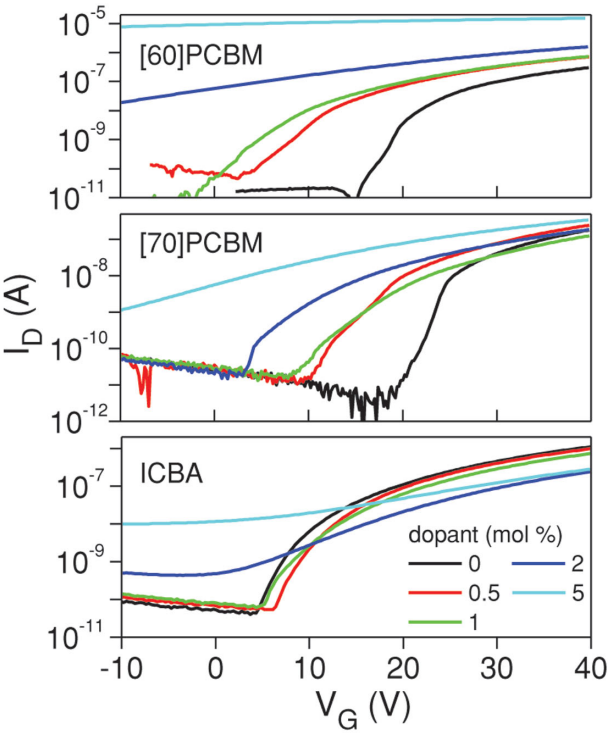

Figure 2. Representative plots of the transfer characteristics in the saturation regime of TFT devices fabricated from fullerene derivatives with the molar concentration of the dopant (N-DMBI) given in the legend. V_D = 40 V for [60]PCBM and [70]PCBM. For ICBA V_D = 120 V. The dimensions of the transistor channel are all W = 1000 µm and L = 40 µm.

effect in [60]PCBM has already been reported previously[27] and was used here as a reference point for n-doping of fullerenes with N-DMBI. From the results shown in Figure 2 we conclude that N-DMBI is also capable of doping [70]PCBM and to a certain extend ICBA. Assuming that the addition of free electrons in the semiconductor channel has a similar effect on the device operating characteristics, one can conclude that the n-doping efficiency of the three substituted fullerenes is a material dependent process, that is, the number of charge carriers donated by the same number of dopant molecules depends on the physical characteristics of the host semiconductor. This is particularly surprising if one considers the fact that some of the tested molecules are characterized by similar electron affinities (i.e., LUMO energies, see Figure S2, Supporting Information).

Close examination of the data in Figure 2 reveals that when [60]PCBM devices are doped with a molar ratio of 5%, the channel OFF and ON-currents increase by ≈6 and ≈1.5 orders of magnitude, respectively. A doping concentration of ≥2% is sufficient to reduce the gate field effect to such an extent that the channel current modulation (i.e., ON/OFF ratio) deteriorates completely with the overall channel conductivity remaining nearly gate field independent for the entire bias range investigated. This dramatic increase in the OFF-current is attributed to the introduction of a large number of free electrons induced by the dopant molecules. Under these circumstances the same gate field is unable to deplete the significantly increased electron charge present across the channel. Therefore, appreciable reduction in the channel current can only be achieved via the application of a significantly larger negative V_G.

In the case of [70]PCBM, the change in the channel current with increasing dopant concentration is much less pronounced than in [60]PCBM transistors. Indicative of this is the fact that the channel OFF-current increases by 3 orders of magnitude while the ON-current only increases marginally by a factor of ≈5. In the case of ICBA devices the current increase is even less pronounced with the channel OFF-current increasing by only 2 orders of magnitude while the ON-current reduces with increasing dopant concentration. It is therefore evident from these measurements that [70]PCBM and ICBA require significantly higher dopant concentrations in order to achieve the same apparent doping effect seen in [60]PCBM devices. This difference is most likely due to the different electronic structures, namely HOMO and LUMO energy levels of each fullerene molecule, and/or to the possible differences in the hydride affinity towards the various fullerene carbon cages, both of which mechanisms will be discussed later.

Similar doping experiments were performed on unsubstituted C_{60} and C_{70} in order to assess the doping efficiency with N-DMBI. To this end we note that although to date there are only a handful of reports on solution grown C_{60} TFTs[7,9–11,30] to the best of our knowledge there is none on C_{70} devices processed from solution. **Figure 3** displays the transfer curves measured from C_{60} and C_{70} transistors at different dopant concentrations. It can be clearly seen from these data that the N-DMBI concentration required to induce similar changes in the transconductance of the channel is approximately

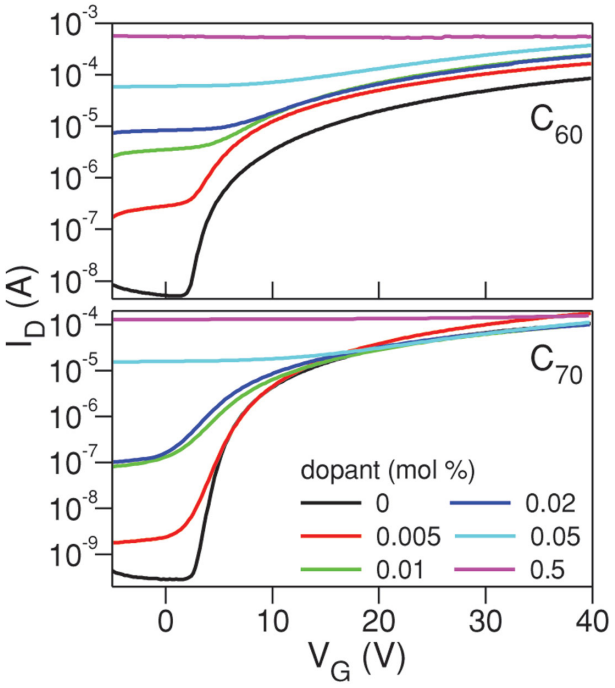

Figure 3. Transfer curves of solution processed C_{60} and C_{70} TFTs in the saturation regime. The molar dopant ratio is given in the legend. Drain voltage V_D = 40 V. The dimensions of the transistor channel are all W = 1000 µm and L = 40 µm.

Table 1. Summary of transistor parameters extracted from the transfer characteristics.

			Electron mobility [cm^2/Vs]		
Dopant c.	0%	0.5%	1%	2%	5%
[60]PCBM	$5.7 (\pm 0.3) \times 10^{-2}$	$5.3 (\pm 0.2) \times 10^{-2}$	$4.7 (\pm 0.1) \times 10^{-2}$	$4.1 (\pm 0.2) \times 10^{-2}$	–
[70]PCBM	$4.6 (\pm 0.5) \times 10^{-2}$	$3.4 (\pm 0.2) \times 10^{-2}$	$1.9 (\pm 0.2) \times 10^{-2}$	$1.6 (\pm 0.3) \times 10^{-2}$	$1.1 (\pm 0.1) \times 10^{-2}$
ICBA	$1.3 (\pm 0.2) \times 10^{-2}$	$1.1 (\pm 0.5) \times 10^{-2}$	$9.9 (\pm 0.4) \times 10^{-3}$	$4.8 (\pm 0.2) \times 10^{-3}$	$4.4 (\pm 0.2) \times 10^{-3}$
C_{60}[a)]	$3.2 (\pm 1.2) \times 10^{-1}$	1.3 (± 0.14)	1.5 (± 0.12)	1.7 (± 0.2)	1.9 (± 0.03)
C_{70}[a)]	$9.4 (\pm 1.7) \times 10^{-1}$	1.8 (± 0.05)	1.4 (± 0.1)	1.1 (± 0.14)	$7.2 (\pm 0.5) \times 10^{-1}$
			Threshold voltage / V_{TH} [V]		
Dopant c.	0%	0.5%	1%	2%	5%
[60]PCBM	15.7 (± 0.7)	11.4 (± 0.5)	9.8 (± 0.6)	2.8 (± 1)	–
[70]PCBM	19.9 (± 0.6)	17.6 (± 0.3)	19.1 (± 0.3)	14.6 (± 0.3)	5 (± 0.4)
ICBA	11.3 (± 0.6)	12.1 (± 0.3)	13.5 (± 0.2)	18.1 (± 0.2)	16.8 (± 0.9)
C_{60}[a)]	2.2 (± 0.2)	1.5 (± 0.2)	0.9 (± 0.4)	0.6 (± 0.7)	–10.4 (± 1.3)
C_{70}[a)]	3.8 (± 0.5)	3.4 (± 0.3)	2.4 (± 1)	0.6 (± 1.1)	0.4 (± 0.5)
			Channel current ON/OFF ratio		
Dopant c.	0%	0.5%	1%	2%	5%
[60]PCBM	2×10^3	3×10^3	1×10^3	4×10^2	–
[70]PCBM	1×10^3	1×10^3	4×10^2	4×10^2	4×10^1
ICBA	1×10^4	2×10^4	1×10^4	1×10^4	7×10^2
C_{60}[a)]	6×10^3	4×10^2	5×10^1	3×10^1	7×10^1
C_{70}[a)]	3×10^4	2×10^4	1×10^2	8×10^1	1×10^1

[a)] Dopant concentration 1/100.

100 times lower than that in [60]PCBM. Furthermore, in C_{60} devices the OFF-current increases by 4 orders of magnitude while the ON-current by a factor of ≈10. In the case of C_{70} the OFF-current increases by ≈5 orders of magnitude while the on-current remains on similar or slightly lower levels. From these results we conclude that the n-doping efficiency of solution-processed C_{60} and C_{70} with N-DMBI is significantly higher than that measured for [60]PCBM, [70]PCBM and ICBA (Figure 2). **Table 1** provides a summary of the transistor operating parameters averaged over a minimum of 7 devices from which the impact of n-doping can be quantitatively assessed. If one considers the fact that [60]PCBM is characterized by the highest isomeric and fullerene content purity, as compared to both [70]PCBM and ICBA, then it can be argued that the dopability of [60]PCBM is indeed higher than both [70]PCBM and ICBA. For ICBA in particular, the observed doping-like effect may well be due to the presence of fullerene impurities (fullerenes other than ICBA). However, proving whether this is the case would require further work, which is beyond the scope of this study.

A key finding is the dependence of the electron field-effect mobility (μ) on N-DMBI concentration. This rather interesting effect is better illustrated in **Figure 4**a where the electron field-effect mobility for each fullerene derivative is plotted as a function of dopant concentration. For [60]PCBM and [70]PCBM based devices the electron mobility (calculated in the linear regime) is 5.7 (±0.3) × 10^{-2} cm^2/Vs and 4.6 (±0.5) × 10^{-2} cm^2/Vs, respectively. Both values are comparable to previously published data.[31,32] For ICBA the electron mobility

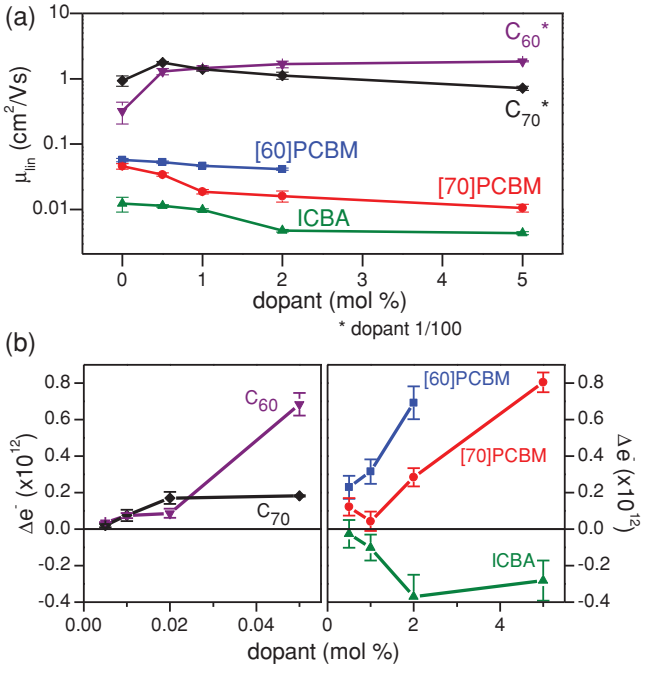

Figure 4. a) Evolution of linear mobility with dopant concentration, note the dopant concentrations for C_{60} and C_{70} are a factor of 100 smaller than for substituted fullerenes b) The additional charge carriers Δe^- added into the channel by the dopant as function of the dopant concentration.

is 1.3 (±0.2) × 10^{-2} cm^2/Vs which is also similar to previously reported results.[32] An interesting observation is that the electron mobility for all three substituted fullerene systems is found to be inversely proportional to the dopant concentration. Indicative of this trend is the fact that at 2% N-DMBI molar ratio the electron mobility drops to 72% of its original value for [60]PCBM, 35% for [70]PCBM and 36% for ICBA transistors. Unlike [60]PCBM, [70]PCBM and ICBA-based devices, C_{60} and C_{70} transistors are found to exhibit a drastically different behavior when doped with N-DMBI. From Figure 4a it can be seen that even at very low dopant concentrations (≈0.005%) the electron mobility increases from 0.32 (±0.12) cm^2/Vs to 1.85 (±0.03) cm^2/Vs for C_{60}, and from 0.94 (±0.17) cm^2/Vs to 1.78 (±0.05) cm^2/Vs for C_{70}. These high mobility values are very interesting if one takes into consideration the fact that the highest electron mobility reported to date for films of C_{70} grown via vacuum sublimation is only 0.06 cm^2/Vs.[33] Furthermore, and to the best of our knowledge, this is the first study in which C_{70} shows higher electron mobility than C_{60}. This is surprising since the electronic structure of unsubstituted C_{60} is known to be isotropic with the LUMO level delocalized over the whole molecule,[34] while in C_{70} it is not since the LUMO level has nodes at 30 of the 70 carbon atoms.[35] Therefore, C_{70} is expected to show lower electron mobility due to increased energetic disorder. However, this simple assumption does not take into consideration important extrinsic effects such as the presence of structural defects, chemical impurities, and so on, which may dominate the long range electron transport measured in field-effect transistors. Nevertheless, from this data it can be concluded that the high electron mobility is a characteristic of C_{60} as well as C_{70}.

In the case of C_{60} the electron mobility is found to increase with increasing dopant concentration. For C_{70} transistors on the other hand the highest mobility was measured at a doping concentration of 0.005% followed by a decrease at higher N-DMBI content. The significant improvement in electron mobility can be attributed to; (i) reduced contact resistance upon doping, and/or (ii) filling of shallow electron traps by dopant-induced free electrons.[36,37] The positive impact of doping on the contact resistance can be seen in the output characteristics of the measured transistors manifested as a linear dependence of I_D on V_D at low bias (Figure S1, Supporting Information). Similar behavior has been observed previously in evaporated C_{60} devices in which the contacts were selectively doped with Rhodocene (also a known n-dopant), leading to an increase in electron mobility from ≈1 cm^2/Vs to ≈2 cm^2/Vs.[38] On the other hand, doping of C_{60} at very low dopant concentrations has also been shown to fill trap states[37] although the impact of n-type doping of the fullerene channel on the macroscopic electron mobility has never been discussed.

The doping efficiency for each fullerene compound was further quantified by analysing the threshold voltage (V_{TH}) shift observed upon doping. By disregarding the charge induced by the dopant molecules, which contributes to the bulk conductivity (and are primarily responsible for the increase in the channel OFF-current), assuming that all remaining free charges are accumulated in close proximity to the interface and disregarding any change in trap density introduced by the positively charged dopant molecules, the total number of donated (i.e., additional) electrons (Δe^-) can be approximated from the shift in V_{TH} using:[39]

$$\Delta e^- = \frac{C_i \left| V_{TH(pristine)} - V_{TH(doped)} \right|}{e}$$

Here, C_i is the geometric capacitance of the gate dielectric and e the elementary charge. According to this model, V_{TH} is the gate potential at which the field induced charge carrier density equals the trap density. Although this simple assumption allows direct correlation of the doping level with the operating characteristics of the device, parasitic effects such as increased trap density due to doping (owed to structural defects), which would lead to underestimating the number of donated electrons, may introduce some error in the calculations. Regardless, such field-effect measurements represent one of the most direct techniques for quantifying the doping efficiency with good accuracy. Finally, since precise calculation of the charge density (i.e., electrons per unit volume), would require detailed knowledge of the electric field profile across the semiconducting film at each position along the transistor channel (information that is difficult to obtain in the presence of dopants), we refrain from estimating this and focus purely on comparing the evolution of V_{TH} between different samples with similar channel geometries.

Figure 4b displays Δe^- as a function of N-DMBI molar ratio (mol%). It can be seen in these plots that in the case of C_{60} and C_{70}, the n-doping process appears to be much more efficient since, compared to n-doping of substituted fullerenes, a nearly 200 times lower N-DMBI concentration is able to induce approximately the same amount of free electrons (Δe^-). A very important observation is that in the case of ICBA the shift in V_{TH} is positive (i.e., shifts towards positive V_G) indicating the introduction of electron traps rather than free (i.e., mobile) electrons seen for all other fullerenes. By comparing the electron mobility dependence (Figure 4a) and the evolution of Δe^- (Figure 4b) with N-DMBI concentration in the case of C_{60} and C_{70}, we conclude that a relatively small amount of free electrons is required to significantly increase the electron field-effect mobility in both C_{60} and C_{70}. This picture is consistent with the scenario of deactivation of energetically shallow electron trap states that are in close proximity to the critical channel interface. Although increasing the dopant concentrations to >0.005 mol% does not appear to further increase the electron mobility, higher N-DMBI concentration leads to a significant increase in the OFF channel current and to complete deterioration of the channel ON/OFF current ratio (Table 1). Unlike C_{60} and C_{70}, incorporation of N-DMBI at any concentration into [60]PCBM, [70]PCBM and ICBA layers is found to reduce the electron mobility in the device. However, and as has already been discussed, in the case of ICBA the electron mobility reduction is accompanied by an increase in the electron trap concentration (evident by the positive V_{TH} shift seen in Figure 2) in the channel rather than the introduction of free (i.e., mobile) electrons, most likely indicating the creation of a significant number of structural defects.

Based on the results presented so far it can be argued that the measured difference in the doping efficiency between the unsubstituted and substituted fullerenes is most likely

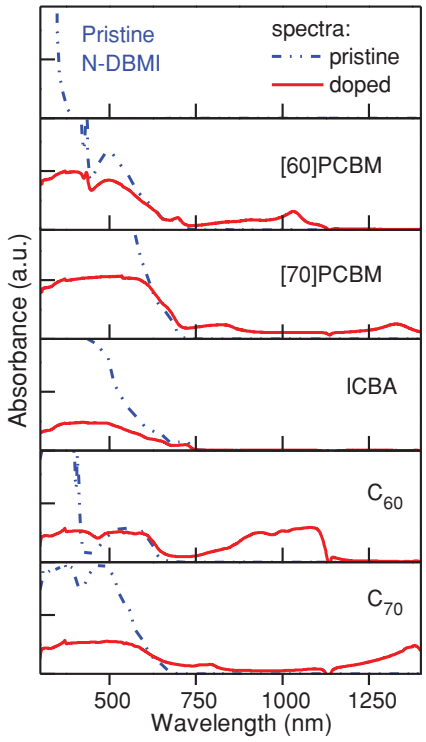

Figure 5. UV–Vis–NIR absorbance spectra of the dopant and dopant semiconductor mixtures measured in solution (CB for N-DMBI, PCBM, ICBA, and DCB for C_{60}/C_{70}). The development of new absorbance peaks upon doping in the near infrared can be accounted to the creation of fullerene anions.

attributed to two main effects; i) differences in the reaction kinetics/energetics of the hydride transfer for each molecule, which is supported by the recent finding of slower reaction kinetics for [60]PCBM than for neat C_{60} in a study of another n-type dopant, namely tetrabutylammonium fluoride, that relies on a similar nucleophilic reaction mechanism;[40] ii) differences in the materials solubility/miscibility, which leads to different degrees of dopant segregation and doping efficiency since segregated dopant molecules are not expected to contribute free electrons to the host semiconductor. Related to the latter effect, it is worth noting that when neat N-DMBI films are incorporated as the channel material in the same transistor structures, no field-induced electron current could be measured. This is to be expected since N-DMBI is by definition a hole transporting material (i.e., facilitates easy hole injection as compared to electrons) due to its very high HOMO level (Figure S2, Supporting Information). Thus in the case of the formation of a phase separated semiconductor/N-DMBI bilayer-like system, we expect no, or very little, contribution to the electron current through the formation of a parasitic N-DMBI parallel channel. Finally, the differences between the electron affinities of different fullerenes might also have an impact since differences between the LUMO levels of substituted and unsubstituted fullerenes do exist (Figure S2, Supporting Information).

To investigate the possible impact of variations in the chemical reaction leading to doping we have studied solutions of each fullerene molecule with N-DMBI via absorption spectroscopy. To achieve sufficient doping a dopant ratio of 50% was chosen with the concentration of the solutions maintained at 0.1 mg/mL in total solids. For the purpose of comparison, important experimental conditions such as time between solution preparation and measurement, was kept constant for all material blend systems investigated. **Figure 5** displays the absorption spectra of neat N-DMBI and the various pristine/n-doped fullerene solutions. Spectra of [60]PCBM, [70]PCBM, C_{60} and C_{70} solutions show the development of a new absorption peak in the near infrared region. The latter lies around 1033 nm for [60]PCBM, 1324 nm for [70]PCBM, 1078 nm for C_{60} and 1380 nm for C_{70}. These additional absorption peaks are attributed to the formation of fullerene anions, which suggests the donation of an electron to the fullerene carbon cage.[29,41] Interestingly, this is not the case for ICBA where no extra absorption peak can be observed in good agreement with the very small, if any, n-doping effect measured from the operating characteristics of ICBA transistors as a function of increasing N-DMBI concentration (Figure 2,4b). Since the ICBA used in this study is characterized by low chemical purity, we speculate that N-DMBI might also react with specific impurities, which in turn would forbid ionization of the fullerene cage. However, because of the very high content of the dopant ratio (50%) used in all solutions, the effect of impurities should not be the determinant factor and signs for significant doping should still be measurable—if n-doping was indeed taking place—something which is clearly not the case as evident from both from the electrical and optical measurements. Another plausible, and very probable, explanation is a lower hydride affinity of ICBA than of neat fullerenes. Such lower affinity may lead to slower reaction kinetics which perhaps forbids the reaction entirely (see argument (i) above). However, detailed study of the mechanism is beyond the scope of this study and will be the subject of future investigations.

The effect of possible dopant segregation was also investigated using atomic force microscopy measurements (AFM) performed on as-cast, pristine and N-DMBI doped fullerene films. **Figure 6** displays high resolution (2 μm × 2 μm scans) AFM topography images of the different fullerene films. Pristine films (top row) appear very flat with a root-mean-square (RMS) surface roughness well below 1 nm. For [60]PCBM, [70]PCBM, ICBA and C_{70} the films surface RMS roughness does not change with dopant ratio. In contrast, C_{60} films feature aggregates—possibly N-DMBI nucleated C_{60} nanocrystals—with an average height of up to 50 nm, which appear in N-DMBI doped samples. The formation of these structures leads to a sharp increase in the RMS surface roughness (Figure S3, Supporting Information). From the AFM data we conclude, with the exemption of C_{60}, that doped and undoped films appear equally smooth and show no indication of significant dopant segregation.

In an effort to further assess the impact of the n-doping process on the overall transistor performance, we have performed gate bias stress stability measurements under inert atmosphere (dry nitrogen). It has previously been shown that the presence of shallow traps within the semiconducting channel deteriorates the bias stability of the transistors.[42] Therefore, deactivation of such trapping states via intentional doping is expected to have a positive impact on bias stability and potentially on long range charge transport within the device. To test

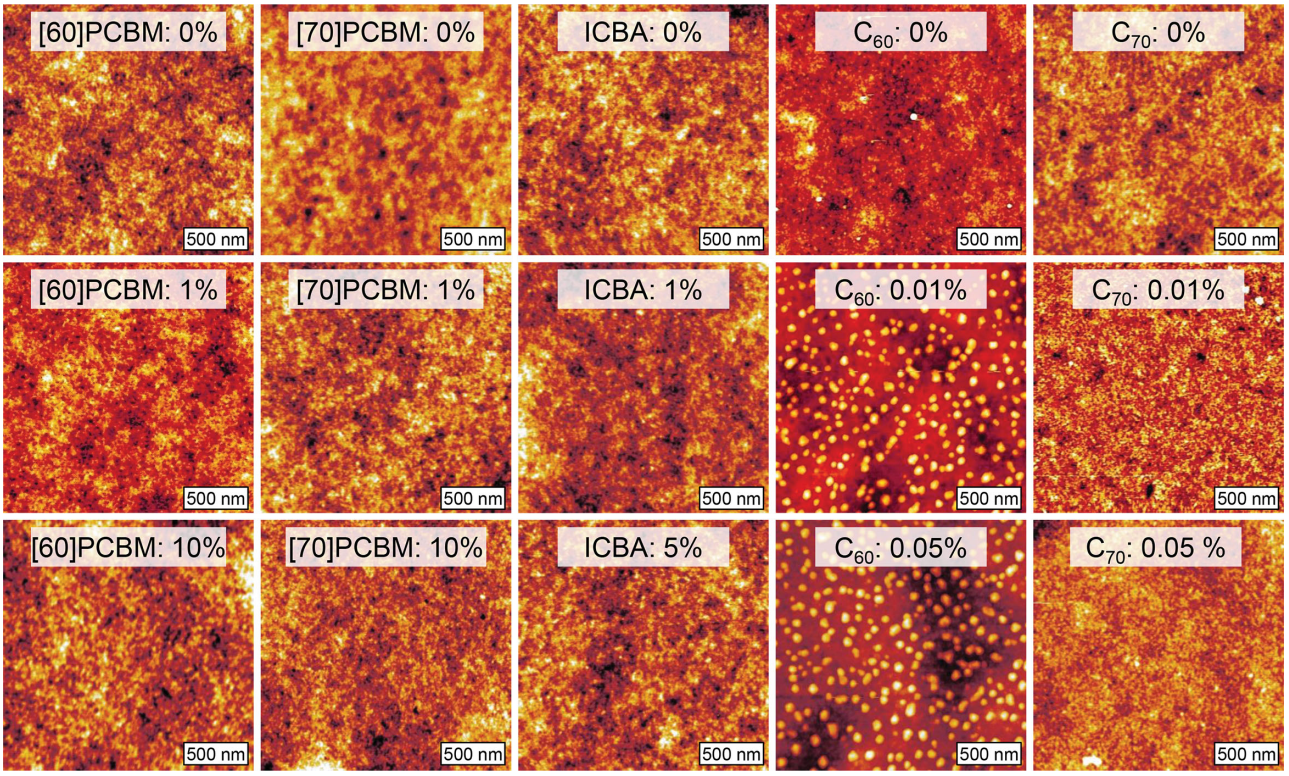

Figure 6. AFM topography images of pristine and doped fullerene films. The size of each scan is 2 μm × 2 μm with the different rows representing films with different doping concentrations (mol%).

this hypothesis we have measured the evolution of the channel ON current (I_D) measured under constant gate and drain bias ($V_G = V_D$ = 40 V for [60]PCBM and [70]PCBM; V_G = 40 V, V_D = 120 V for ICBA; $V_G = V_D$ = 10 V for C_{60} and C_{70}), as a function of bias stress time up to 2 h. **Figure 7** displays the gate bias stress measurements for fullerene transistors at different dopant concentrations. Close examination of the bias stress data reveals a number of interesting characteristics. For example in pristine devices (solid squares), gate bias stressing is found to have a less significant impact on [60]PCBM devices than on [70]PCBM transistors. Specifically, the drain current in pristine [60]PCBM devices decreases by ≈5% while in the case of [70]PCBM transistors we observe a rather dramatic reduction of ≈25% (**Table 2**). Devices based on pristine ICBA exhibit an intermediate bias stress response with the current dropping by approximately 10%. Despite the higher electron mobility, the operating stability of undoped C_{60} and C_{70} transistors appears more sensitive to gate bias stressing. Specifically, the drain current of C_{60} TFTs decreases by approximately 50% and by more than 40% in case of C_{70} transistors. Interestingly, at moderate dopant concentrations (0.1%) the bias stability of the devices [60]PCBM, [70]PCBM and ICBA appears to be comparable to that of the undoped devices (open circles), which is a good indication that the dopant is electrochemically stable once in the blend. At higher doping concentrations (1–2%), the impact of n-doping is found to vary depending on N-DMBI concentration and the specific fullerene derivative used (open triangles). For instance, the bias stability of [60]PCBM devices doped with 1 mol% of N-DMBI is found to be reduced while for [70]PCBM devices this effect appears to be less pronounced. Similarly, ICBA devices become more susceptible to bias stressing at a higher dopant concentration (≥2%). This degraded bias-stress behavior observed in all three substituted fullerenes is consistent with the formation of electron traps upon doping in parallel to creation of free/mobile electrons (Figure 2b), at least in the case of [60]PCBM and [70]PCBM transistors where doping appears to lead to formation of a significant amount of excess electrons. However, this is not the case for ICBA devices where doping appears to induce more traps than free electrons, as evident by the negative value of Δe^-. This interplay of the two competing mechanisms namely the formation of; i) free electrons, and ii) electron traps, is also in qualitative agreement with the decrease in the subthreshold slope (SS) seen in the transfer characteristics of Figure 2 (lower SS value is indicative of higher trap concentration at the interface) as well as with the reduction of the electron mobility as a function of increasing doping concentration (Figure 4a). From these results it can be concluded that doping of the three fullerene derivatives leads to the formation of both free electrons as well as electron traps. Depending of the relative contribution by each process, doping can therefore lead to; i) formation of excess mobile electrons (manifested as a negative shift in V_{TH}) and electron traps (manifested as a reduction in SS), and ii) formation of high concentration of electron traps, that exceeds that of the free electrons induced by the dopant resulting to a positive shift in V_{TH} and in a negative Δe^-. These results demonstrate the versatility of the

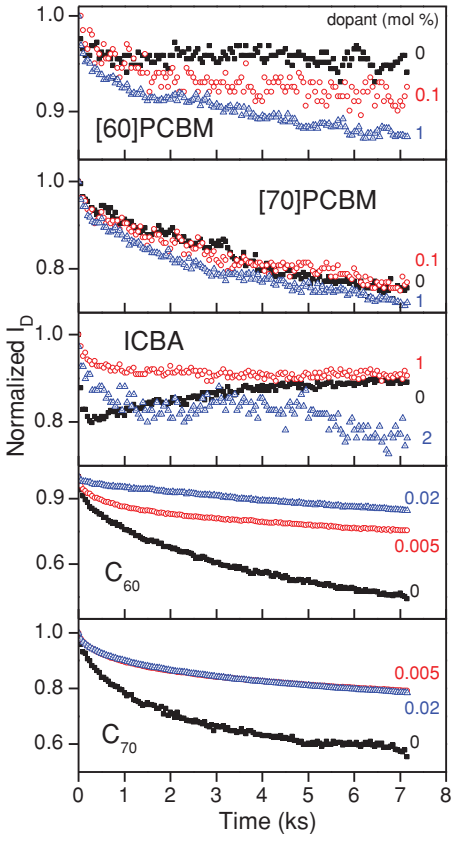

Figure 7. Bias stress measurements obtained for different fullerene-based transistors under the following biasing conditions: $V_G = V_D = 40$ V for [60]PCBM and [70]PCBM; $V_G = 40$ V, $V_D = 120$ V for ICBA; $V_G = V_D = 10$ V for C_{60} and C_{70}.

field-effect measurements as a valuable tool for discriminating between the different doping effects.

Unlike the substituted fullerenes-based devices, doping of C_{60} and C_{70} transistors, even at very low concentrations, is found to significantly improve the overall device bias stability (Table 2). As discussed earlier, this effect is most likely attributed to the filling of shallow electron traps that are present in the pristine films. Although introduction of electron traps –due to structural defects induced by the presence of the dopant molecules– cannot be ruled out, the concentration of dopant-induced mobile electrons (Figure 2b) far outweighs that of the electron traps, leading to an overall positive effect. Therefore, the observed improvement in operating stability of these high electron mobility C_{60} and C_{70} transistors with chemical doping is an important finding as it represents a simple and promising route to the development of high performance solution-processed electronics.

Table 2. Summary of the evolution of the transistor channel current under bias stress for 2 h. Here I_D(0h) indicates the channel current before bias stress, while I_D(2 h) the channel current after continuous bias stress for 2 h. Bias stress measurements were performed in dry nitrogen at; $V_G = V_D = 40$ V for [60]PCBM and [70]PCBM devices; $V_G = 40$ V, $V_D = 120$ V for ICBA devices; $V_G = V_D = 10$ V for C_{60} and C_{70} devices.

		I_D(2 h)/I_D (0 h)	
Dopant [mol%]	pristine	0.1%	1%
[60]PCBM	0.95	0.91	0.88
[70]PCBM	0.75	0.76	0.72
Dopant [mol%]	pristine	1%	2%
ICBA	0.89	0.90	0.77
Dopant [mol%]	pristine	0.005%	0.02%
C_{60}	0.45	0.75	0.84
C_{70}	0.57	0.78	0.78

3. Conclusion

In summary we have studied the influence of n-doping on solution-processed C_{60}, C_{70}, [60]PCBM, [70]PCBM and ICBA using the molecular dopant N-DMBI via a combination of optical spectroscopy and electrical field-effect measurements. Although it is established that N-DMBI is able to n-dope all studied fullerenes, we have demonstrated significant differences in the doping efficiency and overall device operating stability. The n-doping efficiency in unsubstituted C_{60} and C_{70} fullerenes was found to be approximately two orders of magnitude higher than for [60]PCBM, [70]PCBM and ICBA derivatives. This interesting finding contradicts the assumption of a direct electron transfer from N-DMBI to the fullerene molecules[27] and supports the hydride transfer mechanism proposed by Naab et al.[29] Through the use of optimized doping concentrations, we were able to demonstrate solution processed n-channel C_{60} and C_{70} transistors with electron mobilities close to 2 cm^2/Vs. In addition to the beneficial effect of n-doping on electron transport in C_{60} and C_{70}, a significant improvement of the transistor gate bias stability was observed and was attributed to the screening of shallow electron traps by dopant-induced free carriers. The present work highlights a simple and reliable method that can be used for simultaneous optimization of charge transport and device bias stability. We believe that the positive doping effects demonstrated here using this simple doping protocol could be generic and applicable to other material systems.

4. Experimental Section

Transistor Fabrication and Material Processing: Bottom-gate, top-contact (BG-TC) transistors were fabricated using Si^{++}/SiO_2 wafers acting as the common gate electrode and the gate dielectric (400 nm in thickness), respectively. As the hydroxyl groups present in the surface of the SiO_2 are reactive and know to introduce electron trap states at the interface between the gate dielectric and the semiconductor, its surface was passivated by spin coating a thin layer of divinyltetramethyl disiloxane-bis(benzocyclobutene) (BCB) from a 1:20 diluted solution in trimethylbenzene at 3000 rpm followed by a slow ramp-up of 100 °C per hour to 250 °C where it is annealed for 3 h in nitrogen atmosphere. [60]PCBM (99.5% Solvenne), [70]PCBM (99% Solvenne), and ICBA (99% Solvenne), films were spin-cast from 5 mg/mL chlorobenzene (CB) solutions at 2000 rpm in nitrogen atmosphere. The unsubstituted C_{60} (99.5% Sigma-Aldrich),

and C_{70} (99% Solvenne), fullerenes were processed by drop-casting directly onto the Si^{++}/SiO_2/BCB substrates from 5–10 mg/mL 1,2-Dichlorobenzene (DCB) solutions and subsequently vacuum dried at 10^{-5} mbar for 10 min. For the doping experiments, the molecular dopant N-DMBI (98% Sigma-Aldrich) was added to the solution in molar ratios ranging from 0.005% to 5%. After film fabrication the samples are annealed in nitrogen atmosphere for 16 h at 75 °C. Finally, 50 nm-thick Aluminium (Al) top source–drain (S–D) contacts were thermally evaporated directly onto the active layer under high vacuum using appropriate shadow masks.

Transistor Characterisation: The electrical characteristics of as-prepared transistors were measured in nitrogen atmosphere using a 2-channel Agilent B2986 system.

Optical Characterisation: For absorption spectroscopy a Shimadzu UV2600 absorption spectrometer is used. The materials were dissolved in the respective solvents in inert atmosphere and the quartz cuvettes were sealed to avoid oxidation. The time between mixing the solution and recording the spectrum is kept constant for all materials systems at 10 min. The dopant ratio of the doped solution was 50% and the concentration of all solutions was 0.1 mg/mL.

Atomic Force Microscopy Measurements: Atomic force microscopy measurements (AFM) were performed in intermitted contact mode using an Agilent 5500 system in air.

Supporting Information

Supporting Information is available from the Wiley Online Library or from the author.

Acknowledgements

S.R. and T.D.A. are grateful to Engineering and Physical Sciences Research Council (EPSRC) grant number EP/P505550/1 and European Research Council (ERC) AMPRO project number 280221 for financial support. C.M. acknowledges the Swedish Research Council and Formas for funding.

Received: June 5, 2014
Revised: August 13, 2014
Published online: September 10, 2014

[1] B. Geffroy, P. le Roy, C. Prat, *Polym. Int.* **2006**, *55*, 572.
[2] S. Günes, H. Neugebauer, N. S. Sariciftci, *Chem. Rev.* **2007**, *107*, 1324.
[3] H. Klauk, *Chem. Soc. Rev.* **2010**, *39*, 2643.
[4] J. E. Anthony, A. Facchetti, M. Heeney, S. R. Marder, X. Zhan, *Adv. Mater.* **2010**, *22*, 3876.
[5] Y. Zhao, Y. Guo, Y. Liu, *Adv. Mater.* **2013**, *25*, 5372.
[6] T. D. Anthopoulos, B. Singh, N. Marjanovic, N. S. Sariciftci, A. Montaigne Ramil, H. Sitter, M. Cölle, D. M. de Leeuw, *Appl. Phys. Lett.* **2006**, *89*, 213504.
[7] H. Li, B. C.-K. Tee, J. J. Cha, Y. Cui, J. W. Chung, S. Y. Lee, Z. Bao, *J. Am. Chem. Soc.* **2012**, *134*, 2760.
[8] M. Kitamura, S. Aomori, J. H. Na, Y. Arakawa, *Appl. Phys. Lett.* **2008**, *93*, 033313.
[9] C.-F. Sung, D. Kekuda, L. F. Chu, Y.-Z. Lee, F.-C. Chen, M.-C. Wu, C.-W. Chu, *Adv. Mater.* **2009**, *21*, 4845.
[10] W. Kang, M. Kitamura, Y. Arakawa, *Appl. Phys. Express* **2011**, *4*, 121602.
[11] W. Kang, M. Kitamura, Y. Arakawa, *Org. Electron.* **2013**, *14*, 644.
[12] G. Dennler, M. C. Scharber, C. J. Brabec, *Adv. Mater.* **2009**, *21*, 1323.
[13] T. D. Anthopoulos, D. M. de Leeuw, E. Cantatore, P. van 't Hof, J. Alma, J. C. Hummelen, *J. Appl. Phys.* **2005**, *98*, 054503.
[14] E. F. Aziz, A. Vollmer, S. Eisebitt, W. Eberhardt, P. Pingel, D. Neher, N. Koch, *Adv. Mater.* **2007**, *19*, 3257.
[15] B. Lüssem, M. Riede, K. Leo, *Phys. Status Solidi* **2013**, *210*, 9.
[16] X. Zhou, J. Blochwitz, M. Pfeiffer, a. Nollau, T. Fritz, K. Leo, *Adv. Funct. Mater.* **2001**, *11*, 310.
[17] K. Walzer, B. Maennig, M. Pfeiffer, K. Leo, *Chem. Rev.* **2007**, *107*, 1233.
[18] C. K. Chan, A. Kahn, *Appl. Phys. A* **2008**, *95*, 7.
[19] C. K. Chan, F. Amy, Q. Zhang, S. Barlow, S. Marder, A. Kahn, *Chem. Phys. Lett.* **2006**, *431*, 67.
[20] Y. Qi, S. K. Mohapatra, S. Bok Kim, S. Barlow, S. R. Marder, A. Kahn, *Appl. Phys. Lett.* **2012**, *100*, 083305.
[21] B. D. Naab, S. Zhang, K. Vandewal, A. Salleo, S. Barlow, S. R. Marder, Z. Bao, *Adv. Mater.* **2014**, 1.
[22] T. D. Anthopoulos, G. C. Anyfantis, G. C. Papavassiliou, D. M. de Leeuw, *Appl. Phys. Lett.* **2007**, *90*, 122105.
[23] S. Guo, S. B. Kim, S. K. Mohapatra, Y. Qi, T. Sajoto, A. Kahn, S. R. Marder, S. Barlow, *Adv. Mater.* **2012**, *24*, 699.
[24] C. S. Kim, S. Lee, L. L. Tinker, S. Bernhard, Y.-L. Loo, *Chem. Mater.* **2009**, *21*, 4583.
[25] N. Cho, H.-L. Yip, J. a. Davies, P. D. Kazarinoff, D. F. Zeigler, M. M. Durban, Y. Segawa, K. M. O'Malley, C. K. Luscombe, A. K.-Y. Jen, *Adv. Energy Mater.* **2011**, *1*, 1148.
[26] M. Lu, H. T. Nicolai, G.-J.a. H. Wetzelaer, P. W. M. Blom, *Appl. Phys. Lett.* **2011**, *99*, 173302.
[27] P. Wei, J. H. Oh, G. Dong, Z. Bao, *J. Am. Chem. Soc.* **2010**, *132*, 8852.
[28] P. Wei, T. Menke, B. D. Naab, K. Leo, M. Riede, Z. Bao, *J. Am. Chem. Soc.* **2012**, *134*, 3999.
[29] B. D. Naab, S. Guo, S. Olthof, E. G. B. Evans, P. Wei, G. L. Millhauser, A. Kahn, S. Barlow, S. R. Marder, Z. Bao, *J. Am. Chem. Soc.* **2013**, *135*, 15018.
[30] W. Kang, M. Kitamura, T. Itoh, Y. Arakawa, *Jpn. J. Appl. Phys.* **2012**, *51*, 11PD06.
[31] P. H. Wöbkenberg, D. D. C. Bradley, D. Kronholm, J. C. Hummelen, D. M. de Leeuw, M. Cölle, T. D. Anthopoulos, *Synth. Met.* **2008**, *158*, 468.
[32] C.-Z. Li, C.-C. Chueh, H.-L. Yip, J. Zou, W.-C. Chen, A. K.-Y. Jen, *J. Mater. Chem.* **2012**, *22*, 14976.
[33] J. N. Haddock, X. Zhang, B. Domercq, B. Kippelen, *Org. Electron.* **2005**, *6*, 182.
[34] R. C. Haddon, *Acc. Chem. Res.* **1992**, *25*, 127.
[35] R. C. Haddon, *J. Am. Ceram. Soc.* **1996**, *118*, 3041.
[36] S. Olthof, S. Mehraeen, S. K. Mohapatra, S. Barlow, V. Coropceanu, J.-L. Brédas, S. R. Marder, A. Kahn, *Phys. Rev. Lett.* **2012**, *109*, 176601.
[37] S. Olthof, S. Singh, S. K. Mohapatra, S. Barlow, S. R. Marder, B. Kippelen, A. Kahn, *Appl. Phys. Lett.* **2012**, *101*, 253303.
[38] S. Singh, S. K. Mohapatra, A. Sharma, C. Fuentes-Hernandez, S. Barlow, S. R. Marder, B. Kippelen, *Appl. Phys. Lett.* **2013**, *102*, 153303.
[39] G. Horowitz, P. Delannoy, *J. Appl. Phys.* **1991**, *70*, 469.
[40] C. D. Weber, C. Bradley, M. C. Lonergan, *J. Mater. Chem. A* **2014**, *2*, 303.
[41] D. V. Konarev, N. V. Drichko, A. Graja, *J. Chim. Phys. Physico-Chim. Biol.* **1998**, *95*, 2143.
[42] Y. Chen, V. Podzorov, *Adv. Mater.* **2012**, *24*, 2679.